Theor Chem Acc (2006) 116: 641–654
DOI 10.1007/s00214-006-0110-8

REGULAR ARTICLE

A. Ramírez-Solís

The spectroscopy of copper and silver monohalides: what modern quantum chemistry can and cannot do

Received: 7 December 2004 / Accepted: 2 March 2005 / Published online: 2 March 2006

Abstract A comprehensive analysis on the successes and failures of the theoretical spectroscopy of copper and silver monohalides is presented in light of the recent theoretical versus experimental information for these systems. It is shown that although for copper monohalides the standard quantum chemical multireference SCF, perturbational or CI approaches work well to describe their spectroscopy, for their silver counterparts this is not the case always. While density functional theory is intrinsically unable to deal with the most intense transition ($B^1\Sigma^+$–$X^1\Sigma^+$) observed in the whole CuX and AgX series, the CASSCF+CASPT2 method fails for the AgX family is describing this excitation, even with the largest physically meaningful valence orbital active space. The complexity of silver halides arises from the concatenation of three independent problems: first, the isolated atom spectroscopy is much more complex for Ag than for Cu, since for silver the Rydberg $^2P(4d^{10}5p^1)$ state lies close but below the valence $^2D(4d^95s^2)$ one; secondly, the spin-orbit coupling for silver is much larger and thus the fine-structure components of these doublets are intertwined, leading to very large $\Lambda S\Sigma$ mixing effects in the molecular case. Finally, rather strong interactions exist between the numerous $Ag(4d^95s^2)X(np^5)$ and $Ag(4d^{10}5p^1)X(np^5)$ neutral configurations with the $Ag^+(4d^95s^1)X^-(np^6)$ ionic structures, making the accurate description of these mixtures an extremely difficult task, especially for the second $^1\Sigma^+$ state, where even large CASSCF calculations fail at providing continuous state-specific potential energy curves. This remains a true theoretical impasse related to the still unsolved and complex convergence for the coupled CI-orbital multivariate minimization problem. Therefore, it is only possible to properly describe the electronic structure of the excited states of silver monohalides using the full valence active space, to perform variational treatments of the non-dynamic and dynamic electronic correlation treatments with especially optimized and extended RECP-basis sets; then the spin-orbit effects must imperatively be taken into account to qualitatively explain the nature of the observed AgX spectra. However, non-negligible errors are found for some of the basic spectroscopic quantities such as transition energies and vibrational frequencies for the most spectroscopically active excited states.

A. Ramírez-Solís
Laboratoire de Physique Quantique, IRSAMC, UMR 5626 du CNRS, Université Paul Sabatier, 31062 Toulouse Cedex, France.
Depto. de Física, Facultad de Ciencias,
Universidad Autónoma del Estado de Morelos. Av. Universidad 1001 Cuernavaca, Morelos, 62210 México
E-mail: alex@serm.fc.uaem.mx

1 Introduction

The spectroscopy of noble metal monohalides has been studied experimentally for several decades but theoretical studies of systems containing atoms of the third and higher periods call for the most accurate methods of ab initio quantum chemistry. These calculations require new techniques that have to be tested on small systems like diatomics, in order to prove their reliability for properly treating larger systems. This has been achieved since the early 1990s for copper halides while, for the silver monohalide family, this has been possible only in the last few years. The quality of the spectroscopic results strongly depends on the theoretical approach used. In particular, for silver halides, this means that, even qualitatively, the results concerning the nature of the observed excited states is uncertain unless the most sophisticated algorithms for electronic structure are applied. Also, such basic spectroscopic properties as the theoretical vibrational frequencies for the first excited states are completely wrong by factors of 2 or 3 from the experimental values for some of these diatomics. This explains why, by as late as 1995, no theoretical work at all had been devoted to the AgX diatomics. Such a situation is unimaginable for most of the other types of molecules, even for large organic complexes, fullerenes, doped polymers, catalytic sites of enzymes or whole families of chromophores, since these can be extremely well described (from the structural as well as from the spectroscopic point of view) using "standard" ab initio or density functional theory (DFT)-derived methods. This complexity is found, of course, for many other transition metal diatomics.

The situation for noble metal dihalides (MX_2) is even more precarious, since even from the experimental point of view there is little or no information at all concerning CuI_2 and the whole silver dihalide family. From the theoretical point of view, the accurate description of these systems is substantially harder to achieve than for the monohalides for reasons that will be discussed further on.

Molecules of this kind have been detected already 80 years ago. They were difficult to study in the gas phase but new techniques were developed for their production such as high temperature cells, electric discharges or laser ablation of atoms from solid metal in the presence of the dihalogen, making even fine structure investigations at low temperatures feasible. The experimental studies for the monohalides range from the vibrational structure of the lowest electronic states, accurate radiative lifetimes, rotational and hyperfine structure of the observed bands, microwave spectroscopy for the ground and excited states; for some of the dihalides (CuF_2, $CuCl_2$ and $CuBr_2$) laser-induced fluorescence to study rovibrational spectra as well as accurate transition energies from rare-gas matrices for the lowest excited states exist. However, since the aim of this article is to point out some of the outstanding difficulties encountered and failures of the modern quantum chemical methods concerning the spectroscopy of the monohalides, the interested reader is directed to find all the relevant experimental information for the monohalides within the extensive bibliography provided by Guichemerre et al. [1] comprising nearly 60 experimental citations concerning these molecules, except the copper and silver iodides, for which we shall provide the appropriate references.

2 What quantum chemistry has done

2.1 CuX

Copper monohalides have received the most attention from theoreticians since they represent a paradigm of chemical bonding and present the least amount of problems from the computational point of view. A brief panoramic view of the knowledge on this family is due.

The first emission spectrum on CuF was observed since 1925 by Mulliken; then three bands named A,B,C, at 5700, 5060 and 4920 Å were analyzed in the absorption spectrum by Ritschl, and in emission spectra by Woods, improved later by Steele and Broida. A photoelectron spectrum was recorded by Lee and Potts. Ahmed et al. obtained absorption and emission spectra of the five lowest excited electronic states which were assigned to $^3\Sigma^+$, A(0^+, 1), $B\,^1\Sigma^+ C\,^1\Pi$ and D($\Omega = 1$).

Fine and hyperfine structures of these states were also studied and radiative lifetimes were measured. Many theoretical investigations of the ground state were performed ab initio by SCF calculations [2–6], by density functional theory (DFT) [7–10], and by CI, second-order Möller-Plesset perturbational and coupled-cluster (CC) methods [11–14]. The potential energy curves and the spectroscopic constants of the first $^{1,3}\Sigma^+$, $^{1,3}\Pi$, and $^{1,3}\Delta$ excited states have been evaluated using various types of methods to deal with the electronic correlation effects [15–17]. Calculations of the radiative lifetimes of these six excited states were reported [18,19].

The first spectroscopic experiments on CuCl and CuBr were done by Ritschl in 1927, then by Bloomenthal in 1938. In CuCl, six bands (A, B, C, D, E and F systems) were detected. The vibrational structure of these lowest electronic states was analyzed and radiative lifetimes were measured. The rotational and hyperfine structure of these bands was analyzed for CuCl and CuBr. A recent spectroscopic study lead to a reassignment of the excited states of CuCl. Accurate data were obtained by microwave spectroscopy for the ground state of both CuCl and CuBr.

From the theoretical part, the ground state of CuCl was studied by Hartree–Fock (HF) [4,6,13,20] and DFT or CC methods [9,10,21–23]. The excited states were studied by Nguyen et al. [16], Ramírez-Solís et al. [24] and Sousa et al. [25,26]. Radiative lifetimes were theoretically determined by Ramírez-Solís, Daudey, Schamps and Delaval [27–29]. Winter and Huestis [30] performed SCF calculations on CuCl and included spin–orbit interaction semi-empirically using an atoms-in-molecules technique. The ground state of CuBr was studied by DFT calculations [5], and the lowest excited states through MRCI and CC methods [1]; the radiative lifetimes of some excited states were investigated experimentally and theoretically [25,26,31].

For CuI, there are a number of experimental studies (the first one by Mulliken in 1925) concerning the visible spectrum that lead to a tentative identification of the four observed bands arising from the A, C, D and E systems. The E and C systems were confirmed as arising from $^1\Sigma^+$–$X\,^1\Sigma^+$ transitions, while the D system arises from $^1\Pi$–$X\,^1\Sigma^+$ transition. The experimental assignment of the A system was considerably more complicated and took several years to be elucidated; it changed as arising from another $^1\Pi$–$X\,^1\Sigma^+$ transition, to a $^1\Sigma^+$–$X\,^1\Sigma^+$, and back again to a $^1\Pi$–$X\,^1\Sigma^+$ transition (see the experimental bibliography cited in [32]).

However, only two theoretical studies have been done concerning the excited states of CuI. Ramírez-Solís et al. [32] were the first to perform a coupling of highly correlated electronic wavefunctions and include the spin–orbit (SO) effects through the use of an effective Hamiltonian using the optimized MCSCF+CIPSI energies to produce the 18 lowest fine structure states of CuI. Several years later, Sousa et al. [25,26] studied the spectroscopy of CuCl, CuBr and CuI using explicit four-component relativistic calculations where, in a natural way, fine-structure states arise that can be directly compared with the experimental data. However the use of double-group representation imposes some serious constraints from the orbital optimization and CI points of view; thus some drastic measures had to be taken in order to approximately introduce the interaction of ionic and neutral configurations. For the ionic and for the neutral excited states the spinors were optimized without the Cu($4s$). Including the $4s$ orbital introduces two open shells of the same symmetry. This exclusion is really a major inconvenience since this precludes the crucial $3d - 4s$ hybridization

and the Cu(4s)–X(p_σ) mixing which are important for all the $^{1,3}\Sigma^+$ states, but no solution was found since this cannot be handled in the MOLFDIR program package. Nevertheless, in their calculations, the Cu 4s virtual is rather localized and the authors expected the spinors to give a reasonable description of the relative energies of the ionic and neutral excited states. In non-relativistic calculations the molecular states can be assigned using $\Lambda S\Sigma$ coupling. In these relativistic calculations, the intermediate coupling was used, so only the ω and Ω quantum numbers applied. To connect to the previous discussion [32] on the assignment of fine structure states, Sousa et al. [25,26] have analyzed the calculated states in terms of Ω components of $\Lambda S\Sigma$ parent states. The ionic triplet and singlet excited states arise from the $Cu^+(3d^9 4s^1)X^-(ns^2np^6)$ configuration. For these states the halogen is closed shell and the spin–orbit coupling will arise basically from the atomic $Cu^+(3d^9 4s^1)$ splitting (into $^3D_3$, $^3D_2$ and $^3D_1$) which is about 2,000 cm^{-1}; this effect was expected to be the same for all species. However, besides the splitting of the d-orbitals there is also a spin–orbit interaction between states of the same Ω symmetry which allows them to mix. Note that for iodine the ^{2}P SO effects are quite large (around 7,600 cm^{-1}) but these are expected to quench in the molecular states, since the weight of the neutral $Cu(3d^{10}4s^1)X(ns^2np^5)$ component in the active Franck–Condon region is rather small. Both spin–orbit effects have been properly included in [25, 26] and [32].

Guichemerre et al. [1] have recently carried out a systematic MRCI+SO and CC+SO study of the family of monohalides of metals from group I-B, comprising atoms from the second to the sixth row of the periodic table. However, they did not include in their study the CuI and AgI molecules. The importance of relativistic effects and spin-orbit interactions have also been analyzed and compared for this series of molecules in [1]. Their orbital optimization procedure for the excited states was based on the state-averaged version of the CASSCF method and shall be carefully discussed in the following section.

2.2 AgX

Most of the basic research on silver halides is related to the photophysics of the latent image formation, since these molecules are of great practical importance due to their wide use in photographic materials. These molecules are also important from the theoretical point of view since they represent, along with copper and gold halides, a paradigm of chemical bonding in transition metal-containing molecules.

It was in 1927 that Mulliken observed for the first time UV emission of the AgF molecule around 280 nm and pointed out that interactions between the 0^+ states arising from neutral atoms and from Ag^+ and F^- ions were likely to be important. The $B0^+$–$X0^+$ system was found in the 311–343 nm region and was analyzed vibrationally. Much later its dissociation energy was measured. The rotational structure of the two A–X and B–X systems was studied by Clements and Barrow in the late 1960s, who showed that all these states were of the $\Omega = 0^+$ type. One of the most outstanding features of their article was the fact that they suggested that, at variance with the isovalent CuF molecule, these A and B excited states might be predissociated, since their T_{00} transition energy at 29,251 cm^{-1} for the A state is rather close to the dissociation limit of 29,660 cm^{-1}. Some rough sketches of the forms of the potential energy curves of these states were later proposed, but the important new fact they found was that the A state may be a highly anharmonic state, possibly with a potential maximum. However, until 1995, it was not possible to say whether these A and B states arise from electronic states of Σ^+ or Π symmetry, since the theoretical works had until then considered only the ground state [4,9]. By 1993, the last and the most accurate experimental study of the spectrosocpy of AgF was published by Wang and Gole [33] where they reported the discovery, at the fringes of the visible region, of two close and low-lying new excited states (called A′ and a) that are located about 4,300 cm^{-1} below $A0^+$, the state previously known as the lowest excited state. They performed a rotational analysis of the A′ state and concluded that it was an $\Omega = 1$ state, from which they suggested its labeling as A′Ω 1. At the same time, they tentatively assigned the $\Omega = 1$ value for the a state and called it a Ω 1. The radiative lifetimes of the four lowest-lying electronic states were measured to be 7.1 μs (A′), 9.1 μs (a), 240 ns ($A0^+$), and 21 ns ($B0^+$). These lifetimes strongly suggest that the two lowest-lying states are likely to be of triplet character while the two $\Omega = 0^+$ states are of singlet character. So, up to date, only five states are known. The energy difference between the A and B states is only around 2,300 cm^{-1}, a fact that makes it very difficult for theoreticians to elucidate the nature of the corresponding parent states, given the uncertainties already associated with the atomic and ionic fine-structure asymptotes (the errors associated with the IP of Ag and the EA of Cl will be presented later) that might be involved in the diabatic composition of the several states that can be generated for each spin-space symmetry.

From the theoretical point of view, the first study [34] regarding the spectrocopy of AgF appeared. In that article, we reported two-configuration SCF+CIPSI calculations and a semiempirical treatment of the spin–orbit interactions; we also showed that the labeling proposed by Wang and Gole for the a Ω 1 state was inadequate and gave strong theoretical arguments to prove this erroneous assignment. It was concluded that the newly found a and A′ states were actually the $\Omega = 0^-$ and $\Omega = 1$ components of the $^3\Sigma^+$ parent and relabeled them as a $\Omega\, 0^-$ and A′Ω1.

The question of the nature of the electronic parent of the observed $B0^+$ state, responsible for the most intense transition and which is the shortest lived excited state of AgF, was also addressed and we suggested that this state could be correlated with the Rydberg $Ag^+(4d^9 5p^1)F^-(2s^2 2p^6)$ ionic structure. Five years later, in a much more refined study [35], using a large ANO basis set for F, a small-core RECP and a large polarized–optimized valence basis for Ag, we performed extensive CASSCF+CASPT2 calculations for the

seven lowest lying electronic states. These new results clearly showed that the $B0^+$ state is not correlated with the Rydberg ionic structure, as previously proposed; since the $2^1\Sigma^+$ state had been shown to be the $\Lambda S\Sigma$ electronic parent state of the fine-structure $A0^+$ state, and given the difference between the calculated $T_e \sim 1513\,cm^{-1}$ (exp. $\sim$2,300 cm^{-1}) of the $2^1\Sigma^+$ and $^3\Pi$ states, these results pointed to this latter state as the $\Lambda S\Sigma$ parent of the experimental $B0^+$ state. At the CASPT2 level of calculation, the next higher lying state that could contribute ($3^1\Sigma^+$) through spin–orbit couplings to this $B0^+$ state lies more than 8,000 cm^{-1} away. This $^3\Pi$ assignment for the B state, however, was not consistent with the accurately measured radiative lifetimes of 240 ns ($A0^+$), 21 ns ($B0^+$) for the highest-lying excited states, which suggest that the two $\Omega = 0^+$ excited states are of singlet character. Therefore, the first important contradiction between experimental and highly sophisticated ab initio calculations arose for AgF. Later, several other studies appeared but these were concerned only with the ground state of AgF [10,12,14]; the $B0^+$ puzzle still remains since the recent CASSCF+MRCISD+SO and CC+SO calculations of Guichemerre et al. [1] confirmed our previous assignment of the triplet Π state as the parent of this extremely short-lived state.

For the AgCl and AgBr molecules, several rotational analyses were made. AgBr was detected in absorption in 1927 by Frank and Kuhn, and was analyzed vibrationally by Brice. Photoelectron spectra have also been observed [36], and the B state (again the most intense transition) was carefully analyzed [37]. More recently, the B state of both molecules has been studied by fluorescence excitation and mass spectrometry [38]. These studies stressed the lack of knowledge on the nature of the observed transitions for AgCl and AgBr.

From the theoretical part, until very recently, all the studies were only concerned with the ground states: Hartree–Fock [4] and DFT [5,7,9,10,21,22,39,40] calculations were made for AgCl while CASSCF-MRPT2 [41] and DFT [42] calculations were done for AgBr (the molecule and its clusters). It was ony in 2002 that the first ab initio study concerning the excited states of AgCl and AgBr appeared [1] through the use of small-core RECP and spin–orbit optimized potentials for Ag, and small state-appeared averaged CASSCF reference wavefunctions for MRCI calculations of the seven lowest electronic states. A few weeks before that work was submitted, another larger CASSCF+ACPF study, only focused on the accurate spectroscopy of AgCl, was published [43] before [1], but in a different journal. Although this study did not include the SO effects (though they were carefully discussed and predicted on the resulting electronic states, see Sect. III.C of [43]). The essential difference with the approach presented in [1] is that a more physically coherent (but much larger) complete active orbital space (CAS) was used and that full state-specific CASSCF wavefunctions instead of state-averaged ones were used as references for the highly correlated ACPF algorithm. This is actually a key difference when trying to reproduce results that are aimed at comparison with experimental data for the AgX series; this will be explained in the next section.

For AgI the situation is quite meager, both from the experimental as well as from the theoretical points of view. The dissociation energy is 2.20 eV from atomic fluorescence [44], or with the 2.10 eV value from Mulliken [45]; Gaydon gives 2.2 ± 0.3 eV, according to [46]. Five excited states have been so far observed, the A state around 23,900 cm^{-1}, the B state around 31,190 cm^{-1}, the C state around 44,700 cm^{-1}, the D state around 46,000 cm^{-1} and the E state around 47,500 cm^{-1}. It should be stressed that none of these states has been assigned any fine-structure quantum number nor any $\Lambda S\Sigma$ electronic parent, except for the B state, for which a $^3\Pi_{0+}$ assignment has been proposed [46]. We should also say that, contrary to the situation found for AgF where accurate radiative lifetimes are known for all the excited states, no equivalent data regarding AgI are available. This could certainly provide important insight as to the multiplicity of the dominant electronic parents of the experimentally observed states.

Besides their harmonic vibrational frequencies (206, 151, 123, 156, 165 and 130 cm^{-1}, respectively, for the X, A, B, C, D and E states) [47–53] nothing more is known about the higher-lying excited states, neither from newer experiments nor from the theoretical point of view. This lack of experimental information makes the theoretical comparison incomplete and difficult; newer and reliable observations are now needed to fill in the large blank entries in the spectroscopic tables of AgI.

However, a very important work on the B $\leftarrow$ X transitions by Stueber et al. [38] reported fluorescence excitation and mass-resolved excitation spectroscopy (MRES) of jet-cooled AgCl, AgBr and AgI molecules; two hypotheses were put forward to explain the observed AgI, B $\leftarrow$ X transitions between vibrational levels of these two states, one involving a level crossing between two excited states (B/B′) and another with a single complicated excited (B) potential surface. The single B surface was obtained through the Rydberg–Klein–Rees (RKR) fitting method and shows a rather strange shape, like the one seen for the shelf states of the alkali dimers, with a minimum around 5.4 a.u. and a large plateau that extends from 6 to 8 a.u. (see Fig. 8 in that reference). It must be said that a better agreement with the experimental intensities was achieved using a slightly modified B curve in the shelf region, with a local minimum well depth of about 30 cm^{-1} around 7.2 a.u. Nonetheless, neither of these hypotheses gives a fully satisfactory model for what is known as vibrational isotopic splitting.

From the theoretical point of view, until 2003, not a single study had been reported for molecular AgI (although many works exist for the solid); therefore, in [54] we presented equivalent CASSCF(16,12)+ACPF results for the seven lowest states providing benchmark-like potential energy curves that could explain the observed B–X spectra, as had been recently done for AgCl. Since we aimed at comparing our calculated potential energy curves with those provided in [38] through the RKR fitting, it was absolutely essential to obtain curves covering a much larger internuclear range than studied in [34,35,43], so the studied range goes from 4.0 to 20 a.u. Given the previous experience with the CASSCF description

for the excited states of AgCl, for the $2^1\Sigma^+$ state we decided to obtain quasi-state-specific CASSCF(16,12) calculations that could be coherently extended to such long internuclear distances. The best relative weights beyond 5.3 a.u. were found to be 1:7 (0.12, 0.88), which provide an excellent approximation to the true state-specific CASSCF references for the second root of the $^1\Sigma^+$ manifold. This was ascertained by comparing these curves for the region (3.8–5.2 a.u.) where true state-specific solutions could be obtained.

One important fact that is relevant for spectroscopic purposes is that for all states, the weights of the CASSCF reference in the overall ACPF wavefunctions are very similar, around 0.95; this also means that since the size of the singly and doubly excited external spaces are huge compared to the CASSCF wavefunctions, the latter are actually excellent references in all cases.

These results provided a preliminary confirmation of the single-surface hypothesis put forward by Stueber et al. to explain the mass-resolved excitation spectroscopy experiments on the B $\leftarrow$ X transitions, where the RKR fitted excited state potential energy shows a shelf-like curve, with one deep main well and a shallower one at a longer internuclear distance.

The inclusion of the spin–orbit effects in a second step using these highly correlated ACPF energies through the use of an effective spin–orbit Hamiltonian to obtain the fine-structure states that arise from these $\Lambda S\Sigma$ parents was later achieved [55], finally providing solid support for the single B excited surface hypothesis of Stueber et al.

3 Quantum theoretical considerations

3.1 Asymptotic atomic states

It is clear that for molecular calculations to be reliable, before anything else is done, a proper account of the asymptotic atomic states is essential. In particular, a rather accurate positioning is necessary for the ^{2}S–^{2}D and ^{2}S–^{2}P transitions of the metal atoms, for the first ionization potential, for the ^{1}S–^{3}D and ^{1}S–^{1}D transitions of the M^+ ions as well as for the electroaffinity of the halogen in question.

One particular important aspect concerns the inclusion or lack of the scalar relativistic effects (the Darwin and the mass–velocity corrections) which already are crucial for copper. It should be recalled that these scalar effects are large enough to invert, at the Dirac–Fock level, the $3d^{10}4s^1$ and $3d^9 4s^2$ configurations of Cu, placing the latter 900 cm^{-1} below the former. Then, the inclusion of correlation effects upon these relativistic states corrects this wrong ordering. For molecular problems, a more practical approach has been generally adopted through the use of small-core relativistic effective core potentials, that already include the Darwin and mass–velocity scalar relativistic corrections, and large basis sets in conjunction with sophisticated non-dynamic and dynamic electronic correlation treatments; this has been recently achieved using the MRCI, CASSCF+CASPT2, CASSCF+ACPF and CCSD(T) methods for both metals. The complete failure of the large-core 11-active electron Ag RECP [56], both at the CCSD(T) and ACPF levels, has shown explicitly [57] that only small-core RECP with 19-active electrons can accurately reproduce the complex fine-structure spectra for Ag and Ag^+.

Table 1 contains a comparison of the best theoretical and experimental values for the ionization potentials (IP) and excitation energies (T_e) of the metal atoms, as well as of the electron affinity (EA) of the halogen atoms, obtained with different methods (MRCISD, CCSD(T), ACPF) and large ad-hoc optimized valence Gaussian basis sets. The authors of [1] also considered inclusion of the Davidson correction (+Q) in the MRCISD case to take into account the effect of higher-than-double excitations, and determination of excitation energies by means of the equation-of-motion coupled cluster (EOM–CCSD) method [58] for some of the singlet excitations. The theoretical results are compared to the spin–orbit J-averaged (using Landé's rule for the isolated multiplets) experimental values.

Some interesting remarks arise from an analysis of this table. It is clear that the CCSD(T) and CASSCF+ACPF calculations perform better than the multireference methods like the MRCISD+Q, both with absolute errors of less than 800 cm^{-1} for IP values of about 62,000 cm^{-1}. For the transition energies between the ground and excited states T_e of the copper atom and cation, both the CCSD(T) and the ACPF approaches yield excellent results, with errors smaller than 200 cm^{-1} (and 600 for T_e of about 85,000 cm^{-1} for the cation). For the $Cu(3d^{10}4s^1) - Cu(3d^9 4s^2)$ transition, the MRCISD method, even with Davidson's correction, is off by 2,000 cm^{-1} (+Q:1,400 cm^{-1}) for a T_e of 12,000 cm^{-1}, which represents a large error of 16%; this could be explained by the fact that more accurate methods are needed to properly take into account the contribution of higher than double excitations on the differential correlation energy, due to the change of occupation in the 3*d* shell from 10 to 9 electrons. It would appear that the intrinsic size-consistent formulation of the CCSD(T) and ACPF approaches insures a better description of these transitions where a varying number of electrons in the d shell is involved.

For silver, the situation is more complex and the behavior of the CCSD(T) and ACPF differs depending on the transition under consideration. Also, it turns to be a bit surprising that the MRCISD+Q method produces the best estimation for the $Ag(4d^{10}5p^1)$–$Ag(4d^9 5s^2)$ difference around 1,800 cm^{-1}, while the CCSD(T) approach underestimates this difference as 700 cm^{-1} and the ACPF method overestimates it as being 3,000 cm^{-1}. Here the argument of the size-consistency of the CCSD(T) and ACPF versus the approximate inclusion of it by the MRCISD+Q is thus invalidated. The calculated IPs are within 1,000 cm^{-1} from the experimental value for all methods. These purely electronic energies and wavefunctions usually represent the starting point for the consideration of the spin–orbit effects.

A word concerning the brand new multiconfiguration Dirac–Hartree–Fock pseudopotentials for Cu and Ag [61]

Table 1 Best theoretical transition energies and ionization potentials for Cu and Ag in wavenumbers, experimental J-averaged values, halogen electroaffinities in electron volts

Atomic state	MRCISD/+Q[a]	CCSD(T)[a]	CASSCF+ACPF[b]	Exp.*
$Cu^+(^1D:3d^9 4s^1)$	81133/85408	84924[c]	88020	88634
$Cu^+(^3D:3d^9 4s^1)$	77585/80972	84763 (83626)[d]	84360	84958
$Cu^+(^1S:3d^{10})$	58551/60164	62019	61510 (IP)	62310
$(Cu\,^2P_0:3d^{10}4p^1)$	29679/30647	31211	30816	30618
$(Cu\,^2D:3d^9 4s^2)$	9919/10645	11855 (10715)[d]	11836	12019
$(Cu\,^2S:3d^{10}4s^1)$		0		0
$Ag^+(^1D:4d^9 5s^1)$	100893/102909	103554[c]	102789	107129
$Ag^+(^3D:4d^9 5s^1)$	96538/98634	100328 (99901)[d]	98740	101701
$Ag^+(^1S:4d^{10})$	57261/59197	60487	60103 (IP)	61084
$Ag(^2D:4d^9 5s^2)$	32179/31453	30888 (30006)[d]	31384	32030
$Ag(^2P_0:4d^{10}5p^1)$	28630/29679	30163	28332	30165
$Ag(^2S:4d^{10}5s^1)$	0			0
F (EA:$2p^5$–$2p^6$)	2.99/3.21	3.35	3.34[e]	3.41
Cl (EA:$3p^5$–$3p^6$)	3.38/3.52	3.59	3.44[f]	3.62
Br (EA:$4p^5$–$4p^6$)	3.29/3.41	3.46	–	3.52
I (EA:$5p^5$–$5p^6$)	2.87[f]	2.90[g]	2.91[g]	3.06

* Experimental values from [59]

[a] 19-active electron RECP/contracted basis $[7s6p4d3f2g]$ values from [1]; MRCISD with Davidson's correction noted as +Q

[b] 19-active electron RECP/contracted basis $[7s9p6d2f2g]$ values from [60] for Cu and 19-active electron RECP/contracted basis $[6s5p4d2f]$ from [43] for Ag. CASSCF(11,9) used as references for both atoms

[c] Same as (a) but the EOM-CCSD(T) was used to describe the ^{1} S:$(n-1)d^{10}$–^{1} D:$(n-1)d^9ns^1$ transitions

[d] 19-active electron with new MCDHF-PP/$[6s6p4d3f2g]$ contracted basis values from [61]

[e] ANO-large $[5s4p3d2f]$ contracted basis from [35]. CASSCF(8,4)+ACPF value reported here

[f] 7-active electron RECP/optimized $[5s5p2d1f]$ contracted basis, CASSCF(8,4)+ACPF from [43]

[g] 7-active electron RECP/optimized $[6s7p2d1f]$ contracted basis; CASSCF(8,4)+ACPF from [54]

is due here since, for the $d^{10}s^1$–d^9s^2 and the d^{10}–d^9s^1 transitions where a change in occupation of the d orbitals occurs, they provide less accurate CCSD(T) atomic results using equivalent correlation treatment and basis sets as with the old MWB ones; the authors stress that their new CCSD(T) energies lead to errors that are rather large, up to 2,180 cm^{-1} (see Table 5 of [61]), and explicitly show that only a fully huge uncontracted valence $14s13p10d6f4g4h4i$ basis set can reduce these errors to 1,100 cm^{-1}. However, it is clear that such basis sets cannot be used for highly correlated molecular calculations. The connection of this with the spectroscopy of MX molecules is that all the excited states of these halides are diabatically correlated to the $M^+(d^9s^1)X^-(p^6)$ atomic asymptotes and that, for the silver ones, these are sometimes mixed with the $M(d^9s^2)X(p^5)$ neutral ones. The consequences of these atomic errors on the spectroscopy of the MX families have to be met when trying to obtain accurate enough zeroth order wavefunctions (CASSCF), since it is at that point when the approximate positioning of all the neutral and ionic asymptotes proves to be essential for the adequate mixing of configurations in the delicate balance between competing (IP–EA) with the excitation energies for the metals (atom or ion). Thus, various types of mixings are possible between ionic M^+X^- and covalent MX states that are later described.

3.2 Spin–orbit effects on the isolated atoms

It is clear that if the molecular states that have to be elucidated lie within an energy range that is as small as the SO splittings for Cu or Ag (and their ions), the SO effects will have to be extremely well accounted for in the isolated atoms first before these effects can be safely transferred to the molecular environment.

To place the reader in the appropriate perspective of this section, the fine-structure experimental spectra for Cu, Cu^+, Ag, Ag^+ and the halogen series are shown in Table 2. It can be readily seen that the SO splittings for silver are about twice as large as those found for equivalent multiplet of copper, both for the neutral species and for the ions.

For silver, we have already mentioned that the ^{2} P Rydberg state lies below the ^{2}D one. In this respect, silver is truly a unique case in the whole periodic table. A further complication arises when spin–orbit (SO) effects are considered, since the SO coupling constant for the 4d orbitals is rather large ($\zeta_{4d}(Ag^+) = 1,830\,cm^{-1}$) and, as a consequence, the lowest component (J = 5/2) of the ^{2}D doublet lies just below the highest component (J = 3/2) of the $^2P^0$ doublet, their difference being barely 230 cm^{-1}. These two facts together induce great complexity in the theoretical approach if one aims at spectroscopic accuracy, even for the isolated atom. But extreme care must be taken here to properly define this accuracy. Given our experience with the rather complex molecular spectra for these metal halides, we have chosen to use the pragmatic definition, i.e., by this "spectroscopic accuracy" term we mean that the final computed fine-structure states can unambiguously be associated (through their hierarchical energetic order) to the correct experimental quantum numbers, these being the J value of each component of a given atomic multiplet (recall the above-mentioned ^{2}D–^{2}P

Table 2 Best theoretical spin–orbit splittings versus experimental data

State	Theoretical	Experimental*
$Cu^{(a)}\ ^2S$	0	0
$^2D_{5/2}$	11610	11202
$^2D_{3/2}$	13655 (2045)	13245 (2043)
$^2P_{1/2}$	30730	30535
$^2P_{3/2}$	30981(251)	30784 (249)
$Cu^{+(a)}\ ^1S$	0	0
$^3D_3$	21802	21928
$^3D_2$	22890(1088)	22847 (919)
$^3D_1$	23767(1965)	23998 (2070)
$^1D_2$	25987	26264
$Ag^{(b)}\ ^2S$	0	0
$^2P_{1/2}$	29574	29552
$^2P_{3/2}$	30416(842)	30472 (920)
$^2D_{5/2}$	28547	30242
$^2D_{3/2}$	32849(4302)	34714 (4472)
$Ag^{+(b)}\ ^1S$	0	0
$^3D_3$	36,867	39164
$^3D_2$	38466(1599)	40741 (1577)
$^3D_1$	41477(3011)	43739 (2998)
$^1D_2$	44885	46045
F ($^2P_{3/2}$–$^2P_{1/2}$)	-	404
Cl ($^2P_{3/2}$–$^2P_{1/2}$)[c]	912	881
Br ($^2P_{3/2}$–$^2P_{1/2}$)[c]	3739	3685
I ($^2P_{3/2}$–$^2P_{1/2}$)	7738[c], 7610[d], 7580[e]	7603

* Experimental values from [59]

[a] From [60]. ESOP-Diagonal effective Hamiltonian elements, CASSCF+ACPF energies

[b] From [56]. ESOP-Diagonal effective Hamiltonian elements, CASSCF+ACPF energies

[c] Optimized-level Dirac–Coulomb–Fock from [61]

[d] Averaged-level Dirac–Coulomb CISD from private communication with E. Fromager, L. Vischer, L. Maron and C. Teichteil. $4s4p4d5s5p$ shells as active space

[e] ESOP diagonal effective hamiltonian elements from CASSCF+ACPF energies, [54]

All energies in wavenumbers. For an easier assessment of the theoretical SO effects, differences within multiplets are given in parentheses

fine-structure mixing in Ag), or the Ω value for the molecular cases.

For the treatment of the SO term in the electronic Hamiltonian, there are several different approaches, ranging from the treatment of an all-electron four-component Dirac equation [63], or an approximate two-component reduction of this equation [64] to more approximate but more versatile scalar descriptions followed by additional calculations for the SO splittings [65,66].

In a conventional two-step method, the SO coupling is taken into account after the correlation treatment. This has the main advantage to allow a CI process in non-relativistic symmetries, and then to use the most sophisticated and extended CI calculations. Moreover, the use of both RECP techniques and effective Hamiltonian methods, considerably reduces the size of the total Hamiltonian, generally expressed on the basis of correlated LS (or ΛSΣ for linear molecules) states. However, the main drawback here is to use only contracted multiconfigurational wavefunctions, or in other words, to exclude the effects of the SO interaction on the correlated wavefunctions. One can, in principle, overcome this difficulty by introducing in the matrix representation of the total Hamiltonian buffers of highly excited states which have to be computed (at a much higher cost) even if they are not searched for.

Another way to accurately take into account a strong SO effect on a correlated wavefunction is to treat in a one-step method correlation and spin–orbit coupling simultaneously at the same level [64]. However, such a treatment is found to be very demanding computationally and does not allow the best possible CI treatment due to the loss of nonrelativistic symmetries; this method must be avoided for complex problems like the spectroscopy of copper and silver halides.

The EPCISO algorithm [67] keeps the advantages of both types of the previously mentioned methods. It uses an effective Hamiltonian method in a two-step way, and in this manner allows extended as well as sophisticated electronic correlation treatments. This point is crucial for the spectroscopy of silver, as pointed out previously. The effects of the SO coupling on the correlated wavefunctions is taken into account by introducing in the total Hamiltonian, expressed in a determinantal basis, all the single excitations from a given reference space which are important for the SO coupling (via an energy threshold). The reference CSF space is chosen in such a way that only the states of interest are represented; this can be done in a somewhat poor representation since the correlation effects have already been accurately introduced through the effective Hamiltonian technique. In this way, the polarization effects of the SO interaction due to higher-lying configurations on the lower correlated states are taken into

account. In the complex case of Ag, where the fine-structure components of the silver ^{2}D and ^{2}P states are intertwined, this procedure presents a great advantage since it leads to accurate fine-structure calculations, even though only the LS states of interest have been really computed at the ACPF level [57].

For the Cu, Ag, as well as for the halogen atoms the effective spin–orbit potentials (ESOP) of Stuttgart [68,69] have been successfully used (see the comparison with the latest four-component Dirac–Coulumb correlated calculation for iodine in Table 2). It is worth noting that the SO splittings for the metal ions are also reproduced quite well, in spite of the fact that these ESOPs have been basically derived for the neutral atoms.

The most important thing that can be concluded from the application of the effective Hamiltonian SO calculations is that, even though in [57] we were able to correctly reproduce the $^2P_{3/2}$–$^2P_{1/2}$ splitting as 842 (vs. 920 cm^{-1} exp.) and the $^2D_{5/2}$–$^2D_{3/2}$ splitting as 4,302 cm^{-1} (vs. 4472 cm^{-1} exp.), the relative ordering of these four fine-structure states was found to be critically dependent on the diagonal energies defining the effective Hamiltonian of the EPCISO algorithm. These results show the great difficulty in obtaining the correct $^2P_{1/2}$,$^2D_{5/2}$,$^2P_{3/2}$,$^2D_{3/2}$ mixed experimental ordering for neutral Ag due to the complexity needed to properly deal with the $d^{10}s^n p^m$–d^9s^2 differential correlation effects which, of course, can be properly dealt with at the atomic level (using larger basis sets), but cannot be easily transferred to the molecular problem in complex systems like AgX.

3.3 The molecular states

The spectroscopy of all the CuX and AgX molecules can be explained as transitions from the fine structure states arising from the $^{3,1}\Sigma^+$,$^{3,1}\Pi$ and $^{3,1}\Delta$ parents to the $X^1\Sigma^+(0^+)$ ground states. The extent of the interactions between the M^+X^- ionic and the covalent MX structures depends on the possible mixings of the diabatic, atomic and ionic asymptotes for each M–X couple.

Covalent states: In their ground state, the valence configuration of the metal atom corresponds to the ^{2}S state and the halogen atoms are in their ^{2}P state. The first asymptote is thus correlated only to $^{3,1}\Sigma^+$ and $^{3,1}\Pi$ states. The second asymptote corresponds to the excitation of the metal atom to a ^{2}D or a ^{2}P state. The gap between the ground and the first excited asymptotic state, as well as the nature of this excited state, depends on the metal (^{2}D for Cu and ^{2}P for Ag). In these low-lying asymptotes, the halogens remain in their ground state configuration because their excitation energies are much larger than for the metal. It is then easy to note that these two configurations are asymptotically correlated to a large number of singlet and triplet states: one $^{3,1}\Phi$, a couple of $^{3,1}\Delta$, three $^{3,1}\Pi$, one $^{3,1}\Sigma^+$ and two $^{3,1}\Sigma^-$ for M(^{2}D), and one $^{3,1}\Delta$, two $^{3,1}\Pi$, one $^{3,1}\Sigma^+$ and two $^{3,1}\Sigma^-$ for M(^2P).

Ionic states: The configuration of the lowest ionic asymptotic state is $M^+(d^{10})X^-(p^6)$. The first ionic state is hence of $^1\Sigma^+$ symmetry, as well as the ground covalent electronic state, so they will strongly interact when their energies come close together. This does not happen for the excited states near the ground state equilibrium geometry for CuF, CuCl and CuBr but for CuI this begins to occur, especially for the $^{3,1}\Pi$ ones. For the whole silver halide family, this strong neutral–ionic mixing gives rise to theoretical problems anticipated already by Mulliken in 1937.

Higher ionic excited states $M^+((n-1)d^9ns^1)X^-(np^6)$ correspond to the electronic excitation of the M ion in ^{3}D and ^{1}D states states, which can generate $^{3,1}\Sigma^+$, $^{3,1}\Pi$ and $^{1,3}\Delta$ states.

3.4 The choice of zeroth-order references

There are two issues concerning this point: the definition of the active orbital space that can be used and, the question of whether state-specific or state-averaged CASSCF wavefunctions are used as references for further correlated descriptions.

3.4.1 The choice of the active orbital space

The question of the active orbital space that must be chosen to define the reference wavefunctions is not a minor issue and can have important consequences for spectroscopic purposes. The CASSCF calculations of [1] were somewhat limited, since the authors only included 16 electrons in 10 active orbitals, these being the five nd, the $(n+1)s$ and the $(n+1)p_\sigma$ orbitals of the metals, along with the three $n'p$ of the corresponding halogen atom. Without a doubt, this active set of orbitals adequately generates the complete active space of configurations needed for the description of the lowest excited states of copper and gold halides, but it is insufficient to provide even reasonable zeroth-order CASSCF wavefunctions for the excited states of silver halides, since the Ag(^{2}P^0) + X(^{2}P) asymptotes (which cannot be properly described with this CAS) lie *below* the Ag(^{2}D)+X(^{2}P) ones. Recall that the Ag(^{2}P^0) + X(^{2}P) asymptote is diabatically coupled to $^3\Sigma^+$,$^1\Sigma^+$, $^3\Pi$, $^1\Pi$, $^3\Delta$ and $^1\Delta$ configurations that will strongly interact with those arising from the other excited asymptote, as well as with the lowest ionic ones. The exclusion of both the Ag$(n+1)p_\pi$ orbitals from the active set precludes the mixture of the numerous Ag$(4d^{10}5p^1)$X $(n'p_\sigma^s n'p_\pi^t, s+t=5)$, Ag$(4d_\sigma^x\,4d_\pi^y\,4d_\delta^z 5s^2,\ x+y+z=9)$ X$(n'p_\sigma^s n'p_\pi^t, s+t=5)$ neutral and $Ag^+(4d_\sigma^x 4d_\pi^y 4d_\delta^z 5s^1, x+y+z=9)$ $X^-(n's^2n'p^6)$ ionic structures present in the description of the lowest excited states. So, for the silver halides, the CASSCF(16,10) wavefunctions lack the essential effects brought in by the nondynamic electronic correlation associated with one of the most important diabatic neutral structures needed to provide a good zeroth-order reference for the excited states. The smallest set of active orbitals then has to be composed of 12 orbitals, and must imperatively include the other two $(n+1)p_\pi$ orbitals. This generates much

larger CASSCF wavefunctions, with 17,495 CSF instead of only 187 for the $^1\Sigma^+$ symmetry, and 28,344 CSF instead of only 148 for the $^3\Pi$ one; these larger reference CASSCF wavefunctions generate, of course, much larger MRCI spaces of around 500–800 million CSF [35,43,54], instead of the 10 million considered in [1]. However, only such large variational calculations can provide truly reliable theoretical spectroscopic results for the silver halide molecules.

3.4.2 State-averaged versus state-specific orbital optimizations

Once the previous point has been satisfactorily solved, the second point addresses state-averaged (SA) versus state-specific (SS) orbital optimizations. Our experience is that for these complex spectroscopic problems, the state-averaged description provides even qualitatively wrong behavior of the CASSCF wavefunctions for the $2^1\Sigma^+$ excited states of AgX, which are in all cases involved in the B–X transitions of this family; to illustrate this, Fig. 1 shows a comparison of the SS versus SA descriptions for the two lowest $^1\Sigma^+$ states of AgCl. Two basic spectroscopic quantities calculated after highly correlated ACPF calculations using these two different CASSCF wavefunctions as reference are as follows: $R_e(2^1\Sigma^+) = 4.35$ a.u., $\omega_e = 286\,\mathrm{cm}^{-1}$ for the SS reference and $R_e(2^1\Sigma^+) = 4.43$ a.u., $\omega_e = 326\,\mathrm{cm}^{-1}$ for the SA reference; only the experimental vibrational frequency of $279\,\mathrm{cm}^{-1}$ has been reported to compare these theoretical results. These results highlight the importance of the SS-CASSCF zeroth-order description for spectroscopic purposes. The effect of the SS or the SA description on the transition energies is much less evident, since the dynamic correlation energy can be quite different on each electronic state, even within the same spin-space manifold. In [1] the authors used SA CASSCF(16,10) references, averaging over all the space symmetries only optimizing separately the two different spin situations; doing this rather rough orbital averaging introduced such errors as the ones shown above for the frequency of the $2^1\Sigma^+$ state of AgCl, since they also obtained the $\omega_e = 324\,\mathrm{cm}^{-1}$ MRCISD value.

3.4.3 The Spin–orbit effects in the molecules

For the CuX and AgX families, two levels of complexity in the theoretical approach used must be considered. The first one is to use the purely electronic approximation in the Hamiltonian and to neglect the SO effects on the basis of the smallness of these effects for particular cases; this approximation provided good enough descriptions for most of the observed transitions and the experimental spectra could successfully be explained for CuF [17] and CuCl [24,27]. For CuBr, as was mentioned in the previous section, the double-group relativistic calculations of [25,26] naturally take into account these effects.

However, for CuI, the SO effects arising from both atoms have to be imperatively considered, given the much less

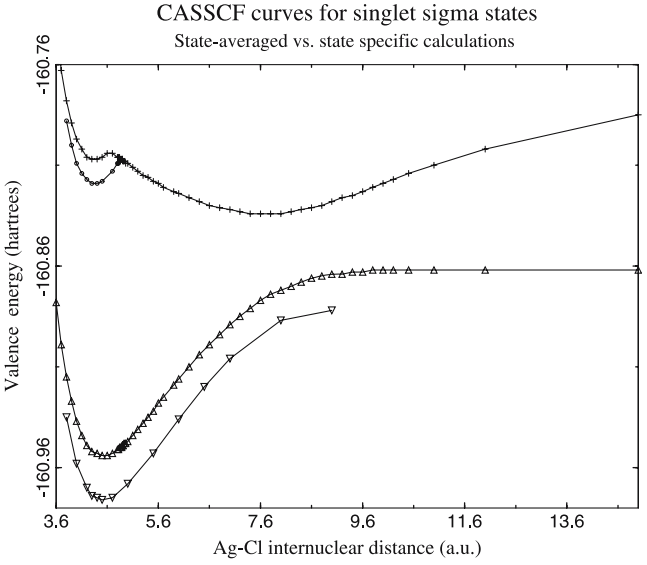

Fig. 1 Comparison of state-specific versus state-averaged (0.5–0.5) CASSCF description for the $X^1\Sigma^+$ and $2^1\Sigma^+$ states of AgCl. Curves are identified by the following notation: state-specific $X^1\Sigma^+$ (*down triangle*); state-specific $2^1\Sigma^+$ (*circle*); state-averaged $X^1\Sigma^+$ (*up triangle*); state-averaged $2^1\Sigma^+$ (*plus sign*). In all cases, 16 active electrons in 12 active orbitals were considered, leading to CAS expansions of 17,945 CSF. Note the divergence problem of the state-specific calculation for the $2^1\Sigma^+$ state beyond 4.725 a.u

evident interplay between the neutral and ionic structures previously discussed. Therefore, the second level of complexity has to be applied, which means that the SO effects are introduced after the electronic description has been achieved. This was done in [32] for CuI.

In the very interesting and careful analysis made in [1] it was shown that for the copper halides, the shapes of the potential energy curves are almost not modified by the spin–orbit interactions. The molecular fine-structure splitting reported is below 0.2 eV, as expected for a $Cu^+(3d^9 4s^1)X^-$ configuration; nevertheless, the interactions between fine structure components are detected, for example, between the $\Omega = 1$ components of $^3\Sigma^+$ and $^1\Pi$ states that leads to the presence of a Q branch and to a substantial Λ-doubling in the $^3\Sigma^+$–$^1\Sigma^+$ system, which are mentioned in a recent experiment [70].

For AgX compounds it has been noted [1] that, as expected from the atomic states, the spin–orbit interactions are about twice as large as for CuX compounds. Strong interactions are expected for these and, as an example, all the different components arising from the parent electronic states are shown in Fig. 7 of [1] for AgF at the minimum of the ground state. Their results for AgX(X = F,Cl,Br) show that the most important interactions are, by far, those arising from the $^3\Pi$ state, between its 0^+ component and the $2^1\Sigma^+$ state, between the $\Omega = 1$ component and the $^1\Pi$, as well as $^3\Delta_1$ states, and a small interaction between the $\Omega = 0^-$ component and the $^3\Sigma_0^+$ state. Another large interaction was found between the $\Omega = 2$ components of the $^3\Delta$ and $^1\Delta$ states, but this is of no consequence to the observed spectroscopy up to date.

For AgI, the same type of SO interactions were found [55], but these effects appear already on top of a more complex situation due to the presence of the double-well $2^1\Sigma^+$ potential that has been previously discussed.

4 Overview: what works fine and what does not

4.1 Equilibrium geometries and harmonic frequencies

Table 3 shows a compilation of the two most basic quantities (equilibrium geometries and frequencies) for which the theoretical results present important deviations. The CuX molecules have been excluded since for these molecules there is better agreement between theory and experiment, therefore, the assignments and the nature of the observed transitions have generally been successfully achieved.

The M–X equilibrium geometries have been measured experimentally (sometimes indirectly) only for the ground states, except very few exceptions, like for the B states of AgCl and AgI. The theoretical MRCI and ACPF values are found in very good agreement (within 0.01–0.015 Å) even without the SO coupling, since the ground states are almost left unchanged by the SO effects. The corresponding MRCISD, CASSCF + ACPF or CC vibrational frequencies are also within 20–30 cm^{-1} from the experimental values for ground states of CuX and AgX. This accuracy has also been very recently achieved through DFT using a hybrid functional [71] for the AgX ground states.

For the excited states, much larger errors exist and the most dramatic failure comes from the pathological behavior of the $^3\Sigma^+$ state of AgI, for which a theoretical CASSCF(16,12) + ACPF value of 867 cm^{-1} has been calculated, while the exp. value is only 151 cm^{-1}. This, of course, stems from the extraordinarily complex mixing of diabatic neutral and ionic configurations that, for this halogen, happens to occur just above the ground state equilibrium geometry (see Fig. 2).

Only for a few of the excited states experimental information exists concerning equilibrium geometries. For instance, for the $B0^+$ state of AgI, the MRES measurements have provided the RKR-fitted values of two potential wells. The ACPF + SO results have provided values (2.52 and 4.29 Å) for both wells that compared with the experience (2.69 and 3.42 Å) are too short and too long, respectively. This problem is coupled to the rather large errors on the corresponding vibrational frequencies, calculated as 351 and 46 cm^{-1}, compared with the 131 and 124 cm^{-1} experimental values for the two minima on this potential. It is quite surprising to find experimentally such a small vibrational frequency for the innermost minimum, which is actually quite close to the repulsive core region of the $B0^+$ state, as can seen in Fig. 2.

Unfortunately, there are still no other studies with which these ACPF+SO values could be compared. Anyway, it is clear that these quasi-state-specific (weights 1:7) CASSCF +ACPF calculations already including the SO effects represent the current state-of-the-art and no other better approach seems possible in the near future for two basic reasons:

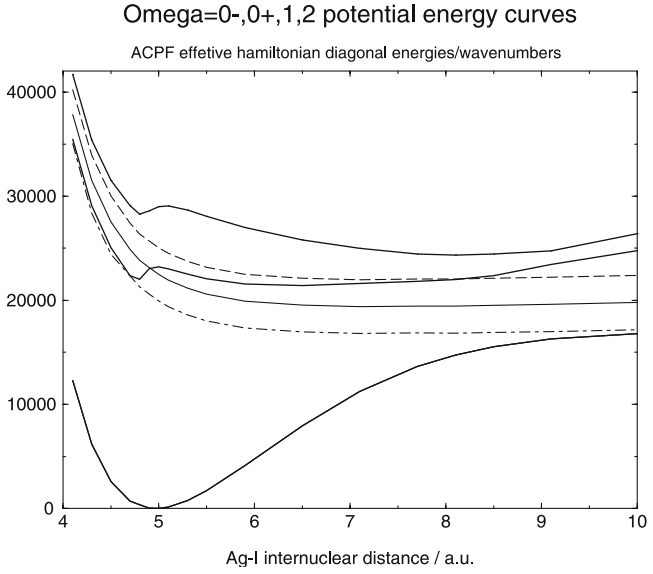

Fig. 2 Potential energy curves for the lowest fine-structure states of AgI in the 4–10 a.u. range. States are identified by the following notation: $\Omega = 0^+$ (*dark full lines*), $\Omega = 2$ (*dotted-dashed curve*), $\Omega = 1$ (*light full line*), $\Omega = 0^-$ (*dashed line*)

(a) A DFT approach is out of the question since this B state contains a dominant component from the $2^1\Sigma^+$ state and, therefore, it cannot be studied with Kohn–Sham based theories. Given the accuracy needed, it seems that time-dependent DFT (TDDFT) is a much too rough approximation to be used for this problem.

(b) The single-reference CC methods are also excluded for the study of such a complex potential since the presence of a maximum near the equilibrium geometry of the ground state clearly shows (see Fig. 2) the strong neutral–ionic configuration mixing that occurs around this spectroscopically active region. So, no better solution for the time being can be envisaged to improve the description already given of this complex $B0^+$ state of AgI.

4.2 Transition energies and nature of the excited states of MX

The spectra of the copper halide family can now almost be fully understood on the basis of the vast experimental and theoretical work. It is very important to point out that the experimental work on radiative lifetimes of the excited states measured from fluorescence decay on CuCl, CuBr and CuI allowed essential insight concerning the singlet and triplet character of the states.

The measured transitions are between the ground state $X^1\Sigma^+$ (from the $Cu^+(3d^{10})X^-(ns^2np^6)$ configuration) and the ionic excited states arising from the $Cu^+(3d^94s^1)$ $X^-(ns^2np^6)$ configuration. Most of the bands in the spectra

Table 3 The most important deviations from experimental values (in parentheses) for some of the basic spectroscopic quantities for AgX

	AgF	AgCl	AgBr	AgI*
$^3\Sigma^+$				
R_e	$1.88^{CASPT2[34]}$, (1.93)	No experiment	No experiment	
ω_e	$553^{MRCI[1]}$, $564^{CC[1]}$ (507)			$867^{ACPF[53]}$ (151)
$2^1\Sigma^+$				$2.52^{[53]}$ $2.56^{[54]}$ (2.69) s
R_e	$1.89^{CASPT2[34]}$, (1.96)	$2.34^{CC-SO[1]}$, (2.32)	–	$4.29^{[53]}$ $4.19^{[54]}$ (3.42) l
		$2.30^{ACPF[43]}$		$532^{[53]}$ $351^{[54]}$ (131) s
ω_e	$523^{MRCI[1]}$, $519^{CC[1]}$ (455)	$324^{MRCI[1]}$, $256^{CC[1]}$ (279)	$216^{MRCI[1]}$ (180)	$74^{[53]}$ $46^{[54]}$ (124) l
$^3\Pi$				
R_e	$2.06^{CC-SO[1]}$, $1.91^{[34]}$ (2.02)	No experiment	No experiment	No experiment
ω_e	$574^{CASPT2[34]}$ (376)			

Bond lengths in angstroms, energies in wavenumbers.
* s and l denote the short and long minima for the $B0^+$ state of AgI

Table 4 Term values (in cm^{-1}) and parent state assignments of the observed excited states of AgX

State	Exp. T_e	Previous Assignment (Ω) New	Theoretical (T_{00} or adiabatic)
AgF			
$A\Omega 0^-$	24931	None $(0^-)^3\Sigma^{+[35]}$	$22773^{CASPT2[35]}$, $25969^{CC+SO[1]}$, $25727^{CC+SO[59]}$
$A'\Omega$ 1	24951	None $(1^{\pm})^3\Sigma^{+[35]}$	$26938^{[34]}$, $22773^{[35]}$, $23630^{MRCI[1]}$, $25969^{CC+SO[1]}$
$A0^+$	29280	None $(0^+)2^1\Sigma^{+[35]}$	$31299^{[34]}$, $27487^{[35]}$, $29598^{MRCI[1]}$, $31130^{EOM-CC[1]}$, $30243^{CC+SO[1]}$, $29195^{EOM-CCSD[59]}$
$B0^+$	31664	None $(0^+)^3\Pi^{[35,1]}$	$28866^{[35]}$, $30969^{MRCI[1]}$, $32421^{CC[1]}$, $33953^{[59]}$ $\{31372(2),31776(1),33792(0^-),34365(0^+)\}^{SO[1]}$
		(1) $^1\Pi^{[59]}$	$34356^{SO[59]}$
AgCl			
B	31606	$^3\Pi(0^+)2^1\Sigma^+$–$^3\Pi$	$31388(2^1\Sigma^+)^{[43]}$, $32098^{MRCI[1]}$, $32663^{EOM-CC[1]}$, $33308(0^+)^{SO[1]}$, $33147^{SO[59]}$
C	43525	None (?) $2^3\Pi$	$43147^{MRCI[1]}$
D	48800	None (2) $^3\Delta^{[43]}$ $(3^1\Sigma^+)^{[1]}$	$50496(^3\Delta)^{[43]}$, $49357(3^1\Sigma^+)^{MRCI[1]}$, $41857^{SO[59]}$
AgBr			
B	31292	None (0^+) $2^1\Sigma^+$	$32663^{MRCI[1]}$, $32340(0^+)^{SO[1]}$, $32501^{SO[59]}$
C	43551	None (0) $(2^3\Pi)^{[1]}$	$43309^{MRCI[1]}$
AgI			
A	23906	None $(0^-, 1)$ $^3\Sigma^+$	$23640^{[54]}$
B	31197	$^3\Pi(0^+)2^1\Sigma^+$–$^3\Pi$	$23230^{[54]}$
C	44720	None (?) $3^1\Sigma^-$	
D	46000	None (?) $2^3\Pi$	
E	47500	None (?) $3^1\Sigma^+$–$3^3\Pi$	

References for the corresponding experimental data are found in each theoretical work cited. T_{00} was calculated using the CASSCF + ACPF energies with zero point energy correction. Experimental Ω values in parentheses

of the heavier copper halides could be assigned to particular excitations in good agreement with experimental data; however, there is still no consensus [25,26] on the interpretation of some of these transitions for CuI, where the presence of the neutral configurations is much more important for the excited states near the equilibrium geometry of the ground state. In the MCSCF + CIPSI calculations of [32] the neutral states, arising from the $Cu(3d^{10}4s^1)I(ns^2np^5)$ configuration, appear in the same energy region as the ionic states, even without the inclusion of spin–orbit interaction. In order to provide definite answers to these questions concerning CuI, more precise CASSCF calculations (using state-specific orbitals for the excited states that correctly take into account this neutral–ionic competition) plus MRCISD-like descriptions are needed now. It should be emphasized that theoretical radiative lifetimes have also been found to be in excellent agreement with experiments for some of these copper halides [27–29].

Table 4 presents the present situation concerning the assignment of the parent states to all the known transitions for the AgX family, as well as the corresponding theoretical transition energies, calculated at various levels of theory.

The use of state-averaged orbital optimization for later correlated applications such as MRCISD has to be properly justified. For some cases, this state-averaged zeroth-order description leads to important qualitative inaccuracies, such as the absence of local maxima and exaggerated harmonic frequencies. For instance, in the AgI case, the double-well B potential cannot be properly obtained using state-averaged CASSCF for the $2^1\Sigma^+$ state.

The large CASSCF(16,12) + CASPT2 calculations for AgF provide transition energies that are off by +2,000 and $-1,700\,cm^{-1}$ for the A and B states. The small CASSCF (16,10)+MRCISD results underestimate by 800–1, $600\,cm^{-1}$ most of the T_e for AgF due to the exclusion of the $5p_\pi$ orbitals from the active space.

In spite of the fact that the state-specific CASSCF + ACPF + EH(SO) method has allowed the confirmation of the one-state hypothesis for the B state of AgI, this very expensive approach yields a transition energy for the $B0^+$ state that is $3{,}000\,cm^{-1}$ below the experimental value of $31{,}197\,cm^{-1}$.

In [1] the authors point out that the largest deviations from experiment arise for dissociation energies, since theoretical values are systematically smaller than experimental data by 0.2 eV on the average. For AgI, the error is also 0.19 eV at the CASSCF + ACPF level [54]. These deviations cannot be explained by the radical change of the diabatic character of the wavefunction ($Cu + F \rightarrow Cu^+F^-$) upon molecular formation, since the energy difference between the covalent and ionic asymptotes is very well reproduced by CCSD(T) and CASSCF + ACPF calculations, with an accuracy better than 0.04 eV. However, some of the experimental D_e values have been indirectly estimated by means of approximate relations.

As a last remark, it should be said that the extremely complex spectroscopy of $CuCl_2$ has been studied and explained using single-reference methods such as SDCI, CPF [72] and CCSD(T) [73]; more recently state-of-the-art benchmark variational multireference methods [60,74] have been applied to study this molecule. However, we have recently shown that DFT-based methods using some of the new and more refined functionals can also provide reliable results, within the ΔSCF approximation, that are of similar accuracy as those painfully obtained with the CASSCF(21,14) + ACPF + SO approach [75]. To our knowledge, this has not yet been attempted for any of the CuX or AgX members and perhaps this approach could provide answers to particular issues that have not yet been solved using standard ab initio methods.

5 Conclusions

This overview of the theoretical works devoted to study the spectroscopy of CuX and AgX molecules has shown that:

1. The multireference second order perturbational scheme (CASPT2) works well to describe the spectroscopy of CuX family but fail rather badly for the AgX series, due to the strong change in character arising from the neutral–ionic configuration mixings that occur for this family. Therefore, these methods should be avoided for this type of molecule.
2. The molecular active orbital spaces have to be carefully defined to include in the zeroth-order reference wavefunctions all the relevant asymptotic neutral and ionic fragments that will interact in the spectroscopically active region.
3. Many of the single-reference coupled-cluster wavefunctions have provided accurate enough results for some (but not all) excited states of these molecules. This is also valid for the EOM-CCSD(T) method for selected singlet excitations.
4. The use of state-averaged orbital optimization for later correlated applications such as MRCISD has to be properly justified and cannot be applied without a careful analysis of its consequences on the spectroscopy; this state-averaged zeroth-order description can lead to important qualitative (such as topological) inaccuracies in the potential curves.
5. The large CASSCF + ACPF approach provides harmonic frequencies for the $2^1\Sigma^+$ and $^3\Sigma^+$ states of AgI that are dramatically overestimated, and in error by up to more than 300 and 500% (over $700\,cm^{-1}$), respectively.
6. Fundamental contradictions remain between the predictions made by small CASSCF(16,10) + MRCISD and CC of [1] and those of large CASSCF(16,12) + ACPF [43], since the former point to the $3^1\Sigma^+$ state while the latter to $^3\Delta_2$ as the parent of the D state in AgCl. It is not clear what other ab initio method could shed new light on this complex problem; the ΔSCF approach of DFT is by nature excluded to deal with such a highly excited root of the $^1\Sigma^+$ manifold and, therefore, it cannot give additional insight.
7. In spite of the fact that the state-specific CASSCF + ACPF + EH(SO) method confirmed the one-state hypothesis of the B state, this very expensive approach yields a transition energy for the AgI $B0^+$ state that is $8{,}000\,cm^{-1}$ below the experimental value of $31{,}197\,cm^{-1}$. Less sophisticated state-averaged CASSCF(+MRCISD) will not provide accurate enough zeroth-order wavefunctions for this complex case. On the other hand, this transition cannot be properly described using single reference methods (CC for example) due to the presence of strong configuration mixing near the ground state R_e; therefore, no other theoretical tool from ab initio quantum chemistry seems able yet to solve this riddle.
8. DFT-based methods (within the ΔSCF approach) using some of the new and more refined functionals can perhaps provide alternative answers to particular questions that have not yet been solved using standard ab initio methods, since many of the transitions can be assigned to de-excitations from states that differ in their $\Lambda S\Sigma$ quantum numbers from the ground states of the CuX and AgX series. TDDFT can be a useful tool to study states of the same spin-space symmetry as the ground state. Also, recent advances in four-component time-dependent DFT [76] will become valuable tools to study the kind of complex spectroscopy found in transition metal dimers.
9. The very recent development of more refined scalar-relativistic and spin–orbit effective potentials has not helped to solve the main problems associated with the excited state description of these molecules, since the new Cu and Ag MCDHF-PP provide less accurate CCSD(T)

atomic results (using equivalent correlation treatment and basis sets as with the old MWB ones) but only for the $d^{10}s^1$–d^9s^2 and the d^{10}–d^9s^1 transitions, where a change in occupation of the d orbitals occurs [61]; the authors stress that their new CCSD(T) energies lead to errors are rather large, up to 2,180 cm^{-1}, and explicitly show that only a huge fully uncontracted valence $14s13p10d6f4g4h4i$ basis set can reduce these errors to 1,100 cm^{-1}. However, it is clear that such basis sets cannot be used for highly correlated molecular calculations. The link of this with the spectroscopy of these MX molecules is that all the excited states of these halides are diabatically correlated to the $M^+(d^9s^1)X^-(p^6)$ atomic asymptotes and that, for the silver ones, these are sometimes mixed with the $M(d^9s^2)X(p^5)$ neutral ones. Unfortunately, they have not included CuI and AgI in their first benchmark applications of these new RECP and SOEP.

10. All in all, the large variety of theoretical efforts to describe the spectroscopy of these molecules has greatly helped obtain important insights to understand the complex spectroscopy of these halides and most of the known transitions have been explained, especially for the CuX family. However, these efforts have also produced fundamental results concerning some excited states that are still far from the experimental ones. Therefore, much work remains to be done to provide new methods which are accurate enough and can properly deal with the essential problems that arise from the nondynamic and dynamic electronic correlation effects on these molecules, since it has been shown that the spin–orbit effects from the atoms (ions) can quite accurately be transferred to the molecules.

Acknowledgements The author thanks PIFI-SESIC(SEP) México and the French CNRS for support during his sabbatical stay at LPQ-IRSAMC.

References

1. Guichemerre M, Chambaud G, Stoll H (2002) Chem Phys 280:71
2. Jeung GH, Barthelat JC, Pélissier M (1982) Chem Phys Lett 91:81
3. Seijo L, Barandarián Z, Klobukowski M, Huzinaga S (1986) Chem Phys Lett 117:151
4. Huzinaga S, Klobukowski M, Barandarián Z, Seijo L (1986) J Chem Phys 84:6315
5. Bowmaker GA, Boyd PDW (1985) J Mol Struct (Theochem) 122:299
6. Miyoshi E, Sakai Y (1988) J Comput Chem 9:719
7. Chen H, Krasowski M, Fitzgerald G (1993) J Chem Phys 98:8710
8. Delley B (1991) J Chem Phys 94:7245
9. Sosa C, Andzelm J, Elkin BC, Wimmer E, Dobbs KD, Dixon DA (1992) J Phys Chem 96:6630
10. van Wüllen C (1998) J Chem Phys 109:392
11. Hrusak J, Tenno S, Iwata S (1997) J Chem Phys 106:7185
12. Laerdahl JK, Saue T, Faegri K Jr (1997) Theor Chem Acc 97:177
13. Mahe L, Barthelat JC (1997) J Mol Struct (Theochem) 401:93
14. Ilias M, Furdik P, Urban M (1998) J Phys Chem A 102:5263
15. Dufour C, Schamps J, Barrow RF (1982) J Phys B 15:3819
16. Nguyen MT, McGinn MA, Fitzpatrick NJ (1986) J Chem Soc Faraday Trans 2(82):1427
17. Ramírez-Solís A, Daudey JP (1989) Chem Phys 134:111
18. Delaval JM, Schamps J (1985) Chem Phys 100:21
19. Schamps J, Delaval JM, Faucher O (1990) Chem Phys 145:101
20. Dixon RN, Robertson IL (1978) Mol Phys 36:1099
21. Ziegler T, Snijders JG, Baerends EJ (1981) J Chem Phys 74:1271
22. Suzumura T, Nakajima T, Hirao K (1999) Int J Quantum Chem 75:757
23. Schwerdtfeger P, Pernpointner M, Laerdahl JK (1999) J Chem Phys 111:3357
24. Ramírez-Solís A, Daudey JP (1990) J Phys B 23:2277
25. Sousa C, De Jong WA, Broer R, Nieuwpoort WC (1997) J Chem Phys 106:7169
26. Sousa C, De Jong WA, Broer R, Nieuwpoort WC (1997) Mol Phys 92:677
27. Ramírez-Solís A, Daudey JP (1990) Phys Rev A 42:5168
28. Delaval JM, Schamps J, Ramírez-Solís A, Daudey JP (1992) J Chem Phys 97:6588
29. Ramírez-Solís A, Schamps J, Delaval JM (1992) Chem Phys Lett 188:599
30. Winter NW, Huestis DL (1987) Chem Phys Lett 133:311
31. Ramírez-Solís A (1993) Phys Rev A 47:1510
32. Ramírez Solís A, Daudey JP, Teichteil C (1990) J Chem Phys 93:7277
33. Wang H, Gole JL (1993) J Chem Phys 98:9311
34. Ramírez-Solís A, Schamps J (1995) J Chem Phys 102:4482
35. Ramírez-Solís A, Daudey JP (2000) J Chem Phys 113:8580
36. Berkowitz J, Batson CH, Goodman J (1980) J Chem Phys 72:5829
37. Patel MM, Nene SG (1982) Indian J Pure Appl Phys 20:247
38. Stueber GJ, Foltin M, Bernstein ER (1998) J Chem Phys 109:9831
39. Nakajima T, Suzumura T, Hirao K (1999) Chem Phys Lett 304:271
40. Nasluzov VA, Rösch N (1996) Chem Phys 210:413
41. Rabilloud F, Spiegelmann F, Heully JL (1999) J Chem Phys 111:8925
42. Zhang H, Schelly ZA, Marynick DS (2000) J Phys Chem A 104:6287
43. Ramírez-Solís A (2002) J Chem Phys 117:1047
44. Terenin A (1930) Physica 10:209
45. Mulliken RS (1937) Phys Rev 51:310
46. Herzberg G (1989) Molecular spectra and molecular structure I Spectra of diatomic molecules, Krieger, Malabar Fla (1989) and references therein numbered 126,780,1374
47. Brice B (1931) Phys Rev 38:658
48. Brice B (1930) Phys Rev 35:960
49. Metropolis N, Beutler H (1939) Phys Rev 55:1113
50. Barrow RF (1948) Proc Phys Soc London 61:99
51. Metropolis N (1939) Phys Rev 636:636
52. Barrow RF, Mulcahy MFR (1948) Nature 162:336
53. Sastry CR, Rao KR (1945) Ind J Phys 19:136
54. Ramírez-Solís A (2003) J Chem Phys 118:104
55. Ramírez-Solís A (2004) J Chem Phys 120:2319
56. Bonacic-Koutecký V, Pittner J, Boiron M, Fantucci P (1999) J Chem Phys 110:3876
57. Ramírez-Solís A, Vallet V, Teichteil C, Leininger T, Daudey JP (2001) J Chem Phys 115:3201
58. Stanton J, Gauss J (1994) J Chem Phys 101:8938
59. Moore CE (1971) Atomic energy levels, NBS Circular No 467, US Govt Printing Office, Washington DC
60. Figgen D, Rauhut G, Dolg M, Stoll H (2005) Chem Phys 311:227
61. Ramírez-Solís A, Daudey JP (2004) J Chem Phys 120:3221
62. Fromager E, Maron L, Teichteil C, Heully JL, Faegri K, Dyall K (2004) J Chem Phys 121:18
63. Vischer L, Saue T (2000) J Chem Phys 113:3996, and references therein
64. Faas S, Snijders JG, Van Lenthe JH, Van Lenthe E, Baerends EJ (1995) Chem Phys Lett 246:632
65. Tilson JL, Ermler WC, Pitzer RM (2000) Comp Phys Commun 128:128
66. Teichteil Ch, Pélissier M, Spiegelmann F (1983) Chem Phys 81:273

67. Vallet V, Maron L, Teichteil Ch, Flament JP (2000) J Chem Phys 113:1391
68. Andrae D, Haussermann U, Dolg M, Stoll H, Preuss H (1990) Theor Chim Acta 77:123
69. Bergner A, Dolg M, Kuechle W, Stoll H, Preuss H (1993) Mol Phys 80:1431
70. Parekunnel T, O'Brien LCO, Kellerman TL, Hirao T, Elhanine M, Bernath PF (2001) J Mol Spectrosc 206:27
71. Kovacs A, Konings RJM (2004) J Phys Chem B 108:8412
72. Bauschlicher CW, Roos BO (1989) J Chem Phys 91:4785
73. Wang XB, Wang LS, Brown R, Schwerdtfeger P, Schröder D, Schwarz H (2001) J Chem Phys 114:7388
74. Ramírez-Solís A, Daudey JP (2005) J Chem Phys 122:14135
75. Ramírez-Solís A, Poteau R, Vela A, Daudey JP (2005) J Chem Phys 122:164306
76. Gao J, Liu W, Song B, Liu C (2004) J Chem Phys 121:6658